Effect of Molecular Weight on Latex Film Formation: Photon Transmission Study

ÖNDER PEKCAN,[1] ERTAN ARDA[2]

[1] Department of Physics, Istanbul Technical University, Maslak 80626 Istanbul, Turkey

[2] Department of Physics, Trakya University, 22030 Edirne, Turkey

Received 14 November 1997; accepted 9 March 1998

ABSTRACT: A UV-visible (UVV) technique was used to monitor the evolution of transparency during film formation from hard latex particles. Two different latex films were prepared from particles with high and low molecular weight (HM and LM) poly(methyl methacrylate) (PMMA) separately and annealed at elevated temperatures in various time intervals above the glass transition temperature (T_g). In both films, a continuous increase in the transmitted photon intensity (I_{tr}) was observed above 160°C as the annealing temperature was increased. However, the reflected photon intensity (I_{rf}) first decreased and then increased by showing a minimum in the same temperature range as the annealing temperature was increased. The increase in the transmitted photon intensity (I_{tr}) is attributed to increase in the "crossing density" at the junction surface. The activation energies for back-and-forth motion (ΔE_{tr}) were measured and found to be around 35 and 25 kcal/mol for the reptating polymer chain across the junction surface in the LM and HM films, respectively. The decrease in I_{rf} was explained by the void-closure mechanism, and the increase in the I_{rf} above 160°C was again attributed to the increase in the crossing density at the junction surface. Back-and-forth activation energies (ΔE_{rf}) were measured to be around 47 and 18 kcal/mol and the void-closure constants (B) were found to be around 24×10^3 and 12×10^3 K for the LM and HM film samples, respectively. © 1998 John Wiley & Sons, Inc. J Appl Polym Sci 70: 339–351, 1998

Key words: latex; film; molecular weight; back-forth motion

INTRODUCTION

Latex films are generally formed by coalescence of submicron polymer particles in the form of a colloidal dispersion, usually in water. The term "latex film" normally refers to a film formed from soft latex particles (T_g below room temperature) where the forces accompanying the evaporation of water are sufficient to compress and deform the particles into transparent, void-free film.[1] However, latex films can also be obtained by compression molding of a film of dried latex powder composed of relatively hard polymers such as polystyrene (PS) or poly(methyl methacrylate) (PMMA) that have T_g above room temperature. Hard latex particles remain essentially discrete and undeformed during drying. The mechanical properties of such films can evolve after all solvent has evaporated by an annealing process which first leads to void closure and then to interdiffusion of chains across particle–particle interfaces.[2]

Film formation from soft- and hard-latex dispersions can occur in several stages: In both cases, the first stage corresponds to the wet initial state. Evaporation of the solvent leads to the second stage in which the particles form a close-packed array; here, if the particles are soft, they

This article is dedicated to the 225th anniversary of Istanbul Technical University.

Correspondence to: Ö. Pekcan.

Journal of Applied Polymer Science, Vol. 70, 339–351 (1998)
 CCC 0021-8995/98/020339-13

are deformed to polyhedrons. Hard latex, however, stays undeformed at this stage. The annealing of soft particles causes diffusion across particle–particle boundaries which leads the film to form a homogeneous continuous material. In the annealing of a hard-latex system, however, deformation of the particles first leads to void closure[1,3] and then the voids disappear and diffusion across particle–particle boundaries starts, that is, the mechanical properties of hard latex films evolve during annealing, after all solvent has evaporated and all voids have disappeared.

After the void-closure process is completed, the mechanism of film formation is known to be the interdiffusion of the polymer chains and the healing of the polymer–polymer interfaces. In general, when two identical polymeric materials are brought into intimate contact and heated at a temperature above the glass transition, the polymer chains become mobile and interdiffusion of the polymer chains across the interface can occur. After this process, the junction surface becomes indistinguishable. This process is called healing

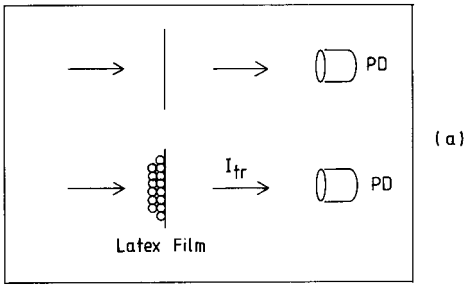

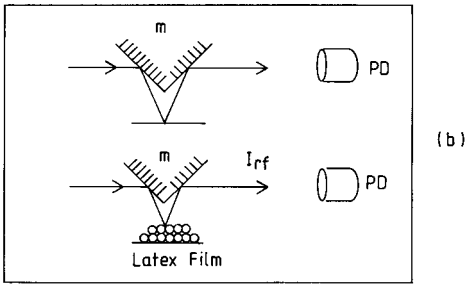

Figure 1 Cartoon representation of (a) UVV spectrophotometer and (b) modified UVV spectrophotometer. PD represents the photodiode and m indicates the triangular mirror system. I_{tr} and I_{fr} are the transmitted and the reflected light intensities, respectively.

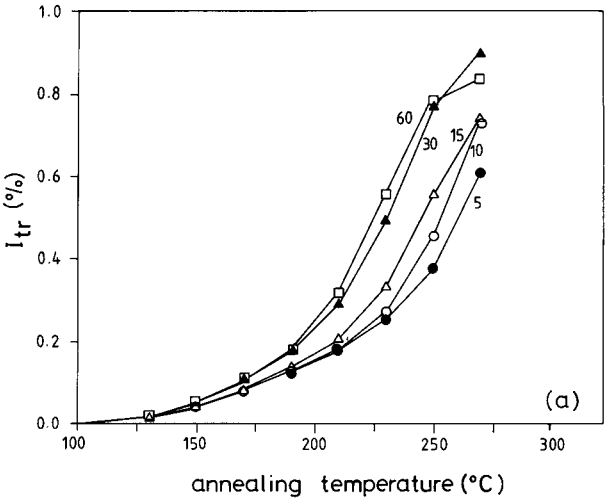

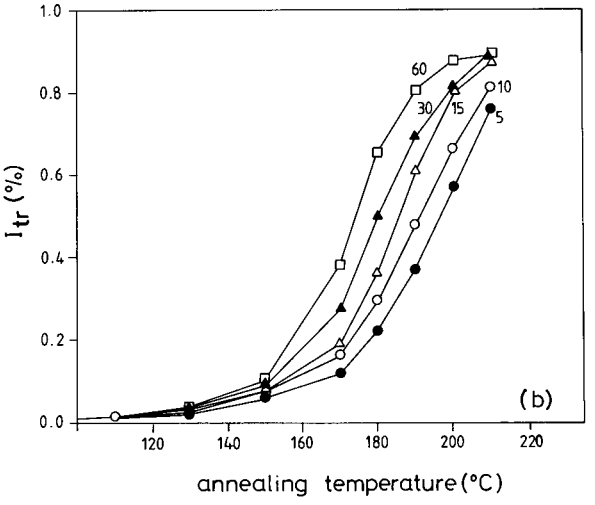

Figure 2 Plot of transmitted photon intensity I_{tr} versus annealing temperature for (a) HM and (b) LM film samples. Nos. on each curve indicate the annealing time intervals.

of the junction at which the joint achieves the same cohesive strength as that of the bulk polymeric material. The word interdiffusion in polymer science is used for the process of mixing, intermingling, and homogenization at the molecular level, which implies diffusion among polymer chains.

Transmission electron microscopy (TEM) has been the most common technique used to investigate the structure of dried films.[4,5] The pattern of hexagons, consistent with face-centered cubic packing, are usually observed in highly ordered films. When these films are annealed, complete disappearance of the structure is sometimes observed, which is consistent with extensive polymer interdiffusion. Freeze-fracture TEM (FF-

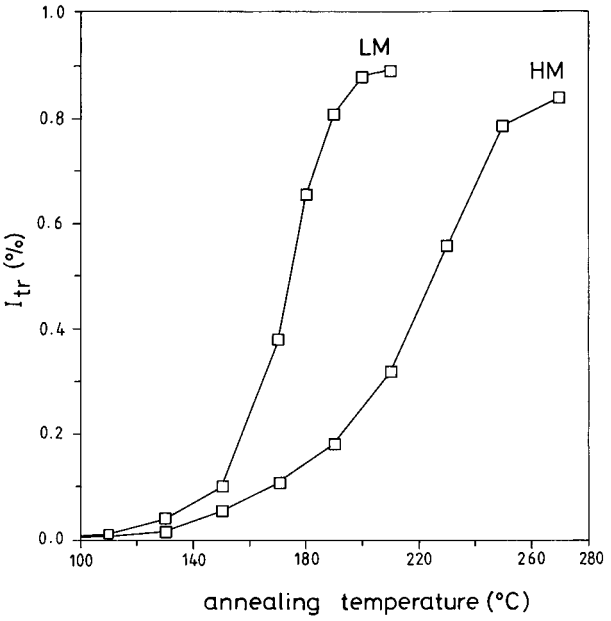

Figure 3 Comparison of transmitted photon intensities I_{tr} versus annealing temperature for HM and LM film samples annealed for 60-min time intervals.

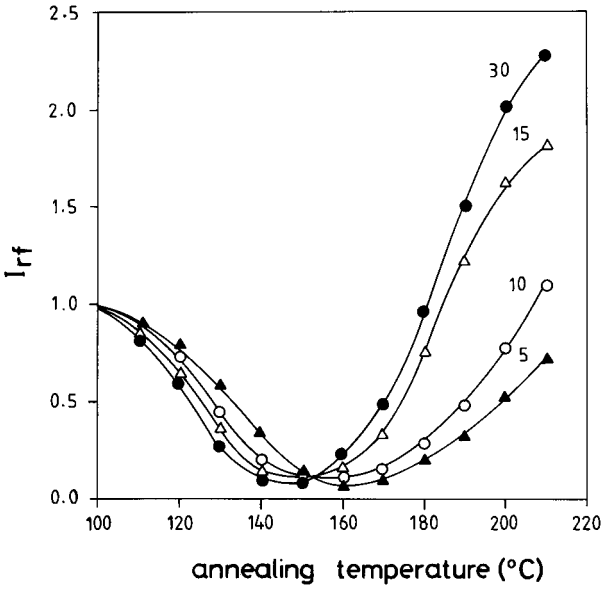

Figure 4 Plot of reflected photon intensity I_{rf} versus annealing temperature for HM films. Nos. on each curve indicate the annealing time intervals.

TEM) has been used to study the structure of dried latex films.[6,7] Small-angle neutron scattering (SANS) has been used to study latex film formation at the molecular level. Extensive studies using SANS have been performed by Sperling and coworkers[8] on compression-molded PS films. The direct nonradiative energy transfer (DET) method has been employed to investigate the film-formation processes from dye-labeled hard[9] and soft[10,11] polymeric particles. The steady-state fluorescence (SSF) technique combined with DET was recently used to examine healing and interdiffusion processes in dye-labeled hard latex systems.[12–16]

In this work, evolution in the transparency of two different latex films formed from particles of two different molecular weight polymers was studied by measuring the transmitted I_{tr} and reflected I_{rf} photon intensities. It was shown that the variation in transparency is related to the variation in I_{tr} and I_{rf} intensities. Latex films were annealed in equal time intervals at elevated temperatures above the glass transition (T_g) of PMMA and I_{tr} and I_{rf} intensities were measured by nonmodified and modified UV-visible (UVV) spectrophotometers, respectively. The increase in the I_{tr} intensity by increasing the annealing temperature was attributed to the increase in the "crossing density" at the junction surface. However, the decrease and increase in I_{rf} were explained by the increase in the void closure and crossing density, respectively, by increasing the annealing temperature during film formation. The method developed by Prager and Tirrell (PT)[17] was employed to investigate the healing

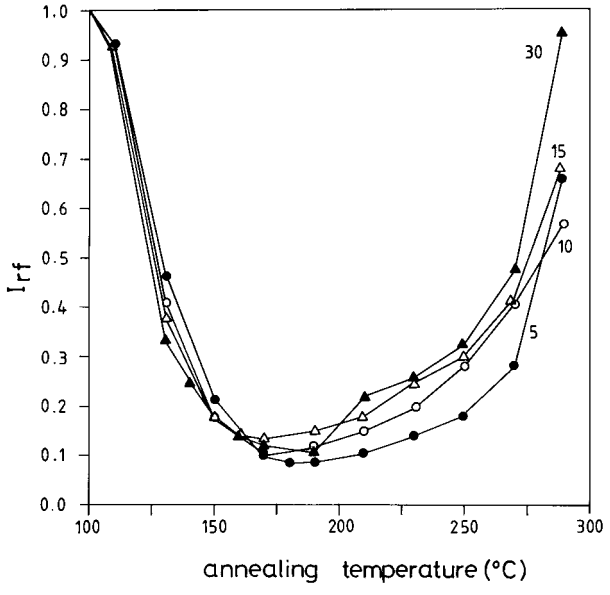

Figure 5 Plot of reflected photon intensity I_{rf} versus annealing temperature for LM films. Nos. on each curves indicate the annealing time intervals.

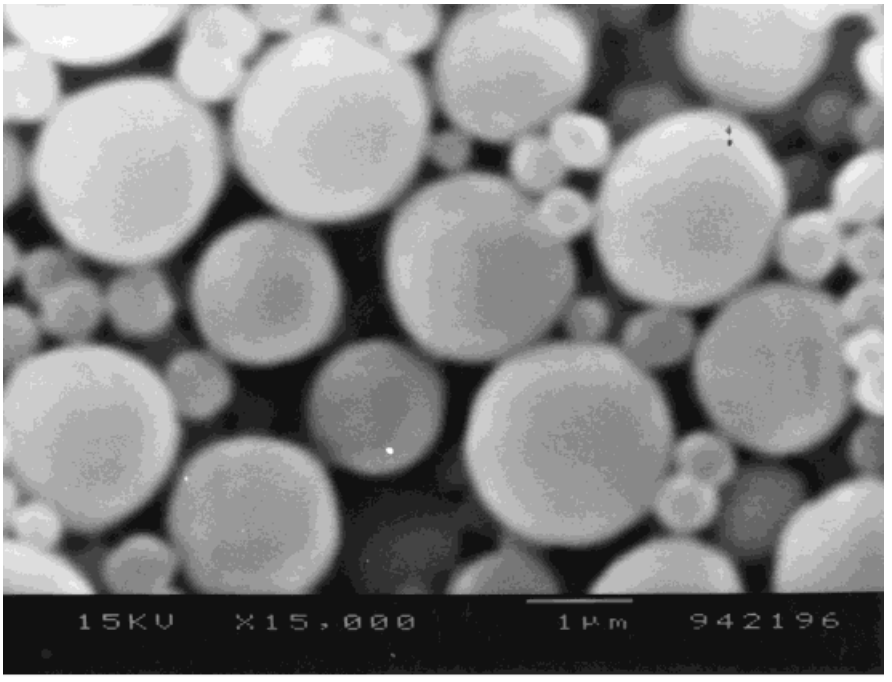

(a)

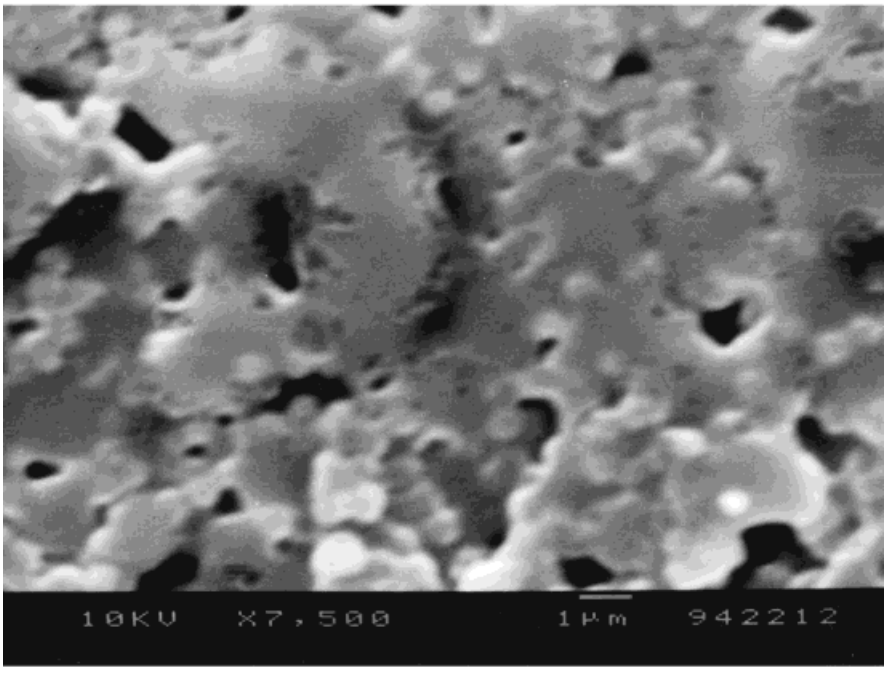

(b)

Figure 6 Scanning electron micrographs (SEM) of latex films: (a) before annealing; (b) annealed at 160°C; (c) annealed at 200°C for 60-min time interval.

processes at the junction surface. Increases in I_{tr} and I_{rf} intensities with respect to the annealing temperature were used to measure the activation energies of the back-and-forth motion for the reptating polymer chains across the polymer–polymer interface.

In all UVV experiments, latex particles having two components were used[18,19]; the major part,

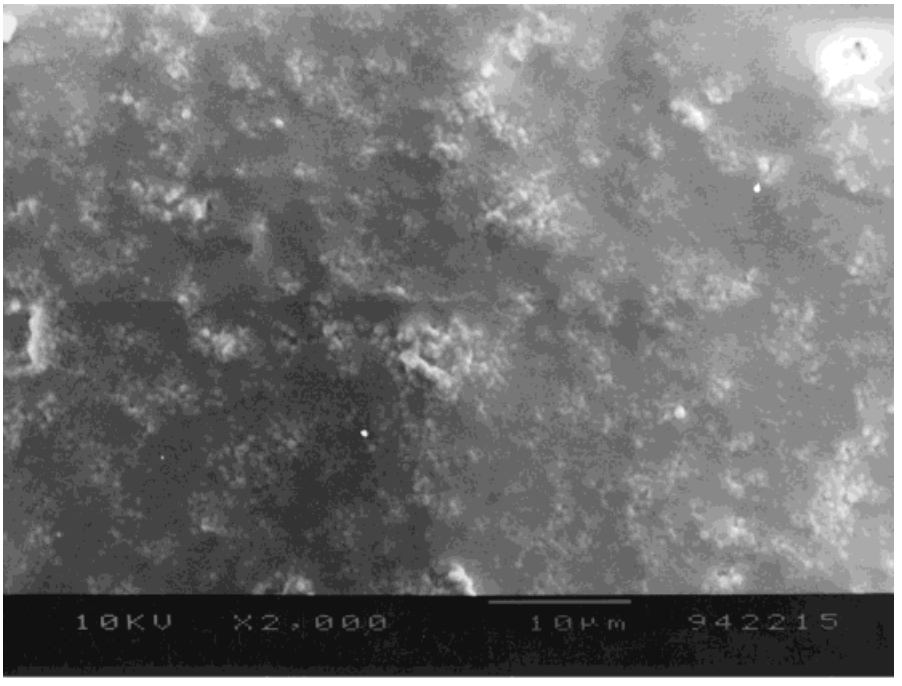

(c)

Figure 6 *(Continued)*

PMMA, composes 96 mol % of the material and the minor component, polyisobutylene (PIB; 4 mol %), forms an interpenetrating network through the particle interior[20,21] that is very soluble in certain hydrocarbon media. A thin layer of PIB covers the particle surface and provides colloidal stability by steric stabilization. Two different films were prepared separately using these PMMA particles with the molecular weights of $M_w = 2.15 \times 10^5$ and $M_w = 1.10 \times 10^5$, respectively.

EXPERIMENTAL

Two different batches of PMMA particles were prepared separately in a two-step process in which MMA in the first step was polymerized to low conversion in cyclohexane in the presence of PIB containing 2% isoprene units to promote grafting. The graft copolymer so produced served as a dispersant in the second stage of polymerization, in which MMA was polymerized in a cyclohexane solution of the polymer. Details have been published.[18] In both batches, stable dispersions of polymer particles were produced, ranging in radius from 1 to 3 μm. Spherical particle sizes were measured from electron micrographs of the particles. A combination of ^{1}H-NMR and UV analysis indicated that these particles contain 4 mol % PIB. (These particles were prepared by Mr. B. Williamson in Prof. M. A. Winnik's laboratory in Toronto.) In the first batch of particles, the molecular weight of graft PMMA was measured as $M_w = 2.15 \times 10^5$, and in the second batch, it was found as $M_w = 1.10 \times 10^5$. The polydispersities of the corresponding PMMA were 1.49 and 2.33, respectively. From now on, these samples will be called HM and LM, which correspond, respectively, to high and low molecular weight PMMA particles. Latex film preparations were carried out by dispersing the PMMA particles in heptane in a test tube with the solid content taken to be 1%. Two different films were prepared from the dispersions of HM and/or LM particles by placing a different number of drops on glass plates of size 0.9×3.2 cm^2 and allowing the heptane to evaporate. Here, we were careful that the liquid dispersion from the droplets has to cover the whole surface area of the plate and remain there until the heptane has evaporated. Samples were weighed before and after the film casting to determine the film thicknesses. The average size for the particles was taken to be 2 μm to calculate the

number of layers in the films. Glass plates were cleaned with acetone after they were used.

In this work, UVV experiments were carried out to measure I_{tr} and I_{rf} from the annealed latex film samples. The annealing process of the latex films was performed in an oven in air above the T_g of PMMA after evaporation of heptane, in 60-, 30-, 15-, 10-, and 5-min time intervals at elevated temperatures between 110 and 270°C for the HM and 110 and 210°C for the LM film samples. The temperature was maintained within ±1°C during annealing. After annealing, each sample was placed in the Lambda 2S Model UVV spectrophotometer of Perkin–Elmer and the I_{tr}'s of the films were detected between 300 and 400 nm. Another glass plate was used as a standard for all UVV experiments. To measure the reflected intensity I_{rf}, from the latex film, a UVV spectrophotometer was slightly modified as presented in Figure 1(b), where two mirrors were placed in triangle position on the path of the light beam, which hits the surface of the film sample to produce the I_{rf} intensity. Figure 1(a) presents the normal UVV spectrophotometer for comparison, which measures the transmitted intensity I_{tr} from the latex film sample. All measurements were carried out at room temperature after the annealing processes were completed.

RESULTS AND DISCUSSION

Transmitted photon intensities from HM and LM films were obtained and are plotted versus the annealing temperature for 60-, 30-, 15-, 10-, and 5-min time intervals in Figure 2(a,b), respectively. It is seen that all the I_{tr} intensity curves increase as annealing temperature is increased. This behavior of the I_{tr} suggests that latex films become transparent to photons as they are annealed. The relatively small I_{tr} intensities observed in the films annealed at short time intervals (5 and 10 min) indicate that some photons dissipate, that is, cannot reach to photodiode after they pass through these films. By increasing the annealing time intervals to 15, 30, and 60 min, the I_{tr} presents larger values as annealing temperature is increased. This behavior of I_{tr} shows that annealing the films in larger time intervals creates more transparent films. When the I_{tr} intensities are compared for the HM and LM samples, it is seen that the HM film needs higher annealing temperatures to reach the same transparency as that of the LM film for the same time intervals. Figure 3 compares the I_{tr} curves for the HM and LM samples for the 60-min annealing time interval.

The reflected photon intensities I_{rf} from the HM and LM film samples, obtained by using the modified UVV spectrophotometer, are plotted versus the annealing temperature for 30-, 15-, 10-, and 5-min time intervals in Figures 4 and 5, respectively. It is seen that all the I_{rf} curves first decreased by showing a minimum, then increased to larger values depending on the annealing time intervals. The initial decrease in I_{rf} is attributed to the homogenization of the film surface due to the void-closure process. In other words, polymeric material flows to fill up the voids between the particles, and as a result, the latex film reflects less photon. However, annealing the film above 160°C reflected that the photon intensity starts to increase and more photons can reach the photodiode as the interfaces starts to heal and disappear. Notice that the HM samples need a higher temperature to produce a reflective surface. This picture can be visualized by taking into account the photon's mean free path $\langle\lambda\rangle$, which is very short at the beginning of the film formation where many interparticle voids exist. At this stage, the films reflect more photons; however, as the film is annealed, interparticle voids start to disappear and $\langle\lambda\rangle$ increases; as a result, I_{rf} starts to decrease. Finally, when all the voids have disappeared, I_{rf} reaches the minima at 160°C where $\langle\lambda\rangle$ becomes the maximum.[22] Above 160°C, after all voids have disappeared, the film gradually becomes a flat mirror. Then, as interfaces heal due to interdiffusion of the chains, the quality of the film (mirror) improves and the film reflects more photons, resulting in an I_{rf} increase. Here, it has to be noted that because of the geometry of the light beam reflected light primarily measures the surface quality of the film; however, transmitted light, which hits the film at a 90° angle, detects the quality of the whole film (see Fig. 1).

To support these findings, scanning electron micrographs (SEM) of the latex films before and after annealing at 160 and 200°C for 60-min time intervals are presented in Figure 6. In Figure 6(a), one can see individual latex particles in powder form of the film where many voids can be observed. However, in Figure 6(b,c), SEM images present the disappearance of interparticle voids and particle boundaries due to the annealing of latex films at 160 and 200°C, respectively, for 60-min time intervals. The film in Figure 6(c) presents higher I_{tr} and I_{rf} intensities than does

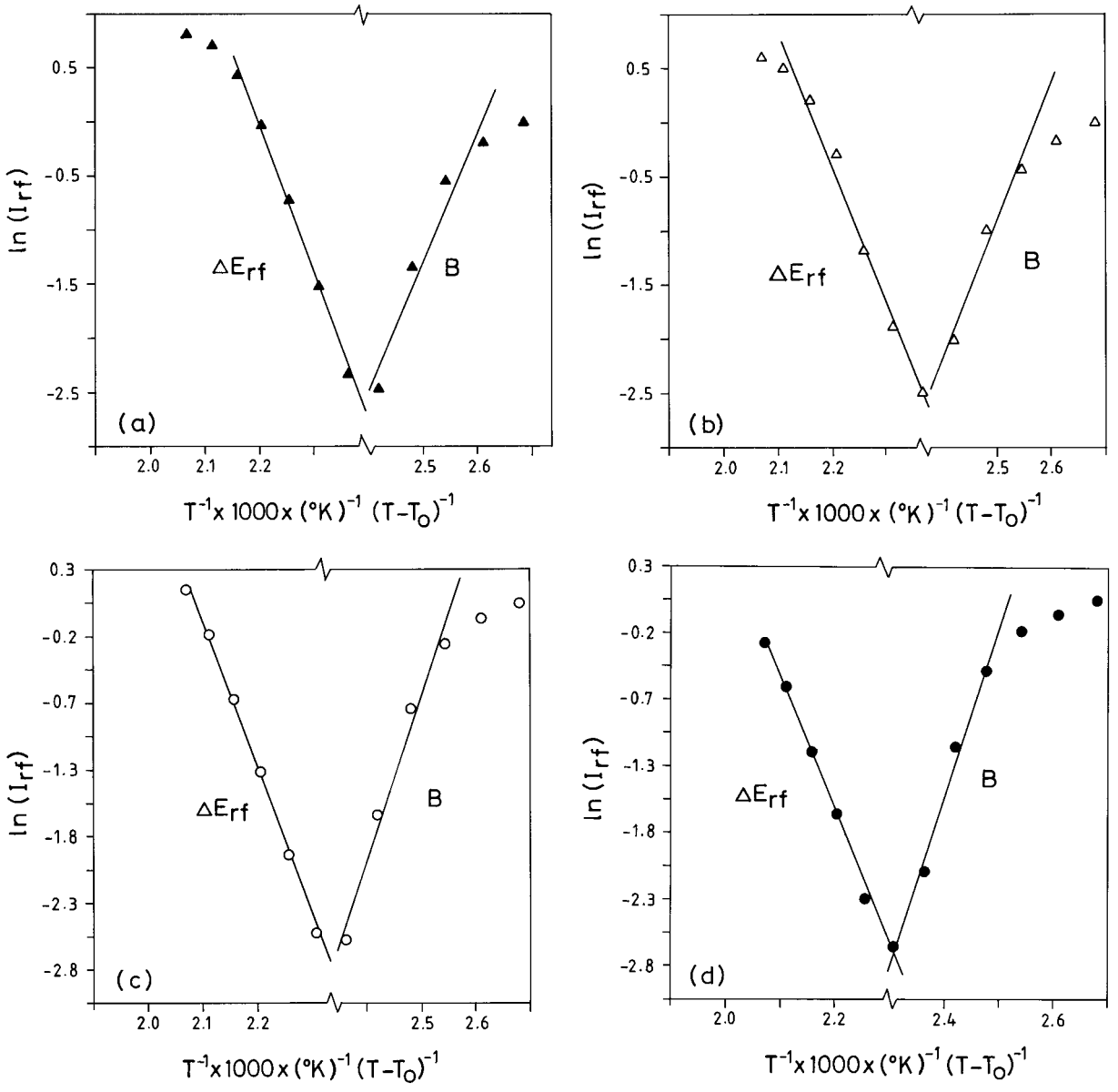

Figure 7 Logarithmic plots of the data in Figure 5 versus reverse of annealing temperature $(T)^{-1}$ and $(T - T_0)^{-1}$ for (a) 30-, (b) 15-, (c) 10-, and (d) 5-min time intervals.

the film in Figure 6(b), indicating that many particle–particle interfaces disappeared due to annealing of the latex film at higher temperature, that is, latex film becomes a high-quality transparent mirror.

Void-Closure Kinetics

To quantify the behavior of I_{rf} below its minima, we introduce the phenomenological void-closure model. The void-closure kinetics can determine the time for optical transparency and film formation.[23] To relate the shrinkage of the spherical void of the radius, r, to the viscosity of the surrounding medium, η, an expression was derived and is given by the following relation[3]:

$$\frac{dr}{dt} = -\frac{\gamma}{2\eta}\left[\frac{1}{\rho(r)}\right] \tag{1}$$

where γ is surface energy; t, the time; and $\rho(r)$, the relative density. It has to be noted that here

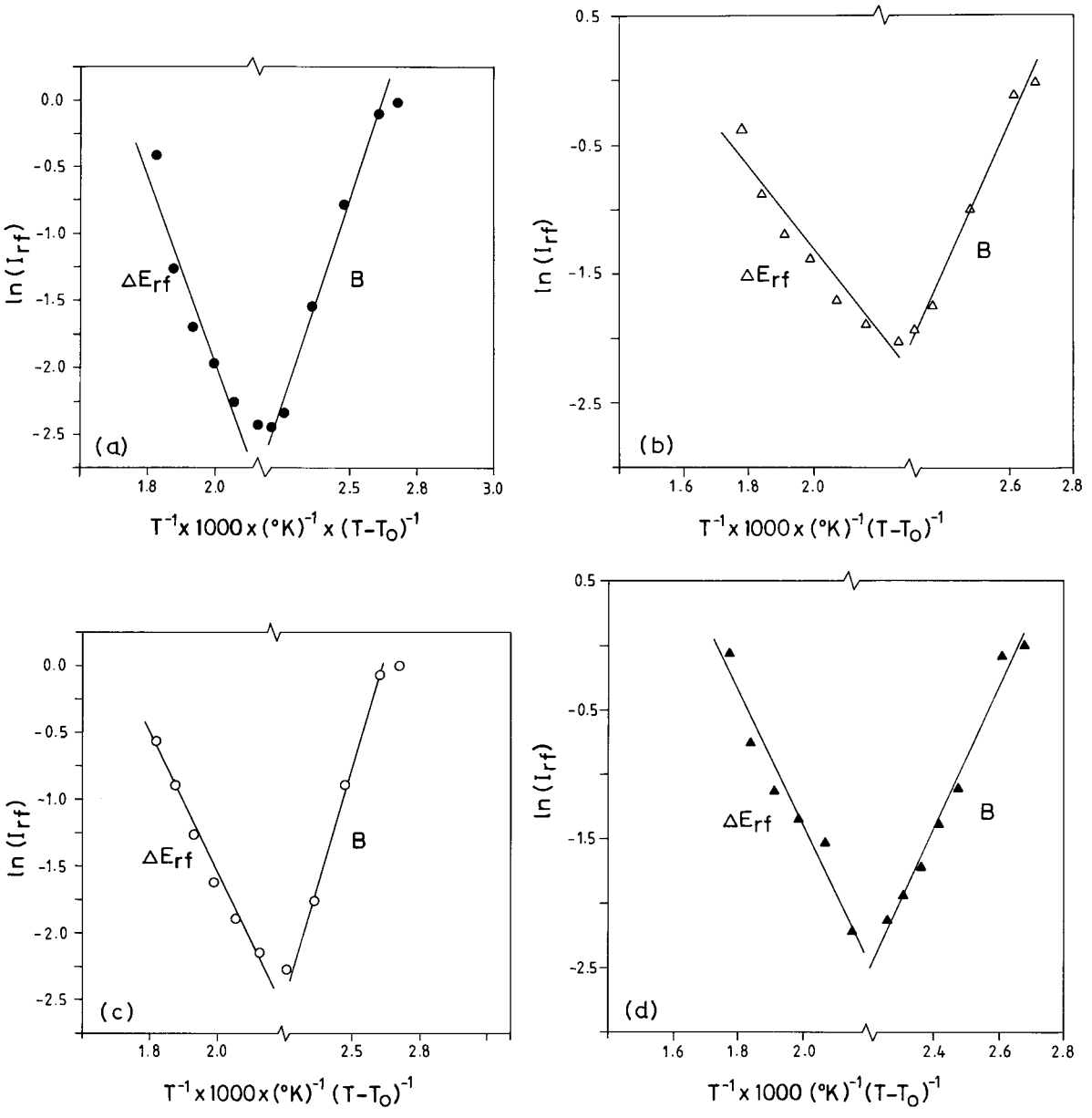

Figure 8 Logarithmic plots of the data in Figure 4 versus reverse of annealing temperature $(T)^{-1}$ and $(T - T_0)^{-1}$ for (a) 30-, (b) 15-, (c) 10-, and (d) 5-min time intervals.

the surface energy causes a decrease in the void size and the term $\rho(r)$ varies with the microstructural characteristics of the material, such as the number of voids, the initial particle size, and packing. Equation (1) is similar to one which was used to explain the time dependence of the minimum film-forming temperature during the latex film formation.[23,24] If the viscosity is constant in time, integration of Equation (1) gives the relation as

$$t = -\frac{2\eta}{\gamma}\int_{r_0}^{r} \rho(r)dr \qquad (2)$$

where r_0 is the initial void radius at time $t = 0$.

The temperature dependence of the viscosity of most of the amorphous polymers near their T_g can be described by the Vogel–Fulcher (VF)[25,26] equation as

Table I Experimentally Measured Values of Back-and-Forth Activation Energies ΔE_{tr} and ΔE_{rf} and Void Closure Contants B for HM and LM Film Samples for Various Annealing Time Intervals

		Annealing Time Interval (min)					
Measurements		60	30	15	10	5	
ΔE_{tr}	HM	26.31	27.68	24.16	23.13	23.12	24.88
(kcal/mol)	LM	37.85	35.16	35.53	32.83	34.85	35.24
ΔE_{rf}	HM		19.7	13	16.57	23.41	18.17
(kcal/mol)	LM		54.3	50.4	43.9	39.95	47.13
$B \times 10^3$ (K)	HM		10.9	11.2	13.6	13.9	12.4
	LM		23.8	25.5	24.6	25	24.72

The last column gives the averaged values. ΔE_{tr} is measured with the unmodified UVV technique and ΔE_{rf} and B are measured with the modified one.

$$\eta = A \exp\left(\frac{B}{T - T_0}\right) \tag{3}$$

where A, B, and T_0 are constants for a given polymer. For most glasses, T_0 is typically about 50 K lower than the T_g. By combining eqs. (2) and (3), the following useful equation is obtained:

$$t = -\frac{2A}{\gamma} \exp\left(\frac{B}{T - T_0}\right) \int_{r_0}^{r} \rho(r) dr \tag{4}$$

Equation (4) will be employed to interpret the data of photon reflection to explain the void-closure mechanism as follows:

When the film samples were annealed for 5-, 10-, 15-, and 30-min time intervals, a continuous decrease in the I_{rf} intensities were observed, until they reached to minimum. To quantify these results, eq. (4) can be used where we assume that the voids are spherical [i.e., $\rho(r) \alpha r^{-3}$]. Then, the integration of eq. (4) produces the relation

$$t = \frac{2AC}{\gamma}\left(\frac{1}{r^2} - \frac{1}{r_0^2}\right) \exp\left(\frac{B}{T - T_o}\right) \tag{5}$$

where C includes the related constants for the relative density, $\rho(r)$.

Here, an assumption can be made that the I_{rf} intensity is proportional to the void radius, r, that is, as voids disappear, the I_{rf} decreases. Then, eq. (5) can be written as

$$t = \frac{2AC}{\gamma} \exp\left(\frac{B}{T - T_0}\right) I_{rf}^{-2} \tag{6}$$

where it is naturally considered that the initial radius of void r_0 is much larger than r, which then resulted in the omission of r_0^{-2} compared to r^{-2}. Equation (6) can be solved for I_{rf} to interpret the experimental results as

$$I_{rf} = S(t) \exp\left[\frac{B}{2(T - T_0}\right] \tag{7}$$

where

$$S(t) = \left(\frac{2AC}{\gamma t}\right)^{1/2} \tag{8}$$

On the right-hand side of Figures 7 and 8, logarithmic plots of I_{rf} versus $(T - T_0)^{-1}$ for the LM and HM films annealed in 30, 15, 10, and 5 min are presented, where ln I_{rf} increased linearly for all samples, which indicates that the model chosen for the void-closure mechanism works well for our UVV data. In other words, the slopes of the right-hand side of Figures 7 and 8 produce B values according to eq. (7). B values are found to be around 12.4×10^3 and 24.72×10^3 K for HM and LM films, respectively, and are listed in Table I. These values are three and six times larger than the values obtained for acrylic (4×10^3 K)[27] and 60 times larger than those was found for water-borne acrylic lattices.[23,28] A smaller value for copolymer of MMA and 2 ethylhexyl acrylate lattices were attributed to the plasticizing effect of water.[23] In our case, no such plasticizing effect is expected, because our PMMA latex has a glass transition of 380 K, which is very high compared to water-borne acrylic lattices ($T_g \approx 280$

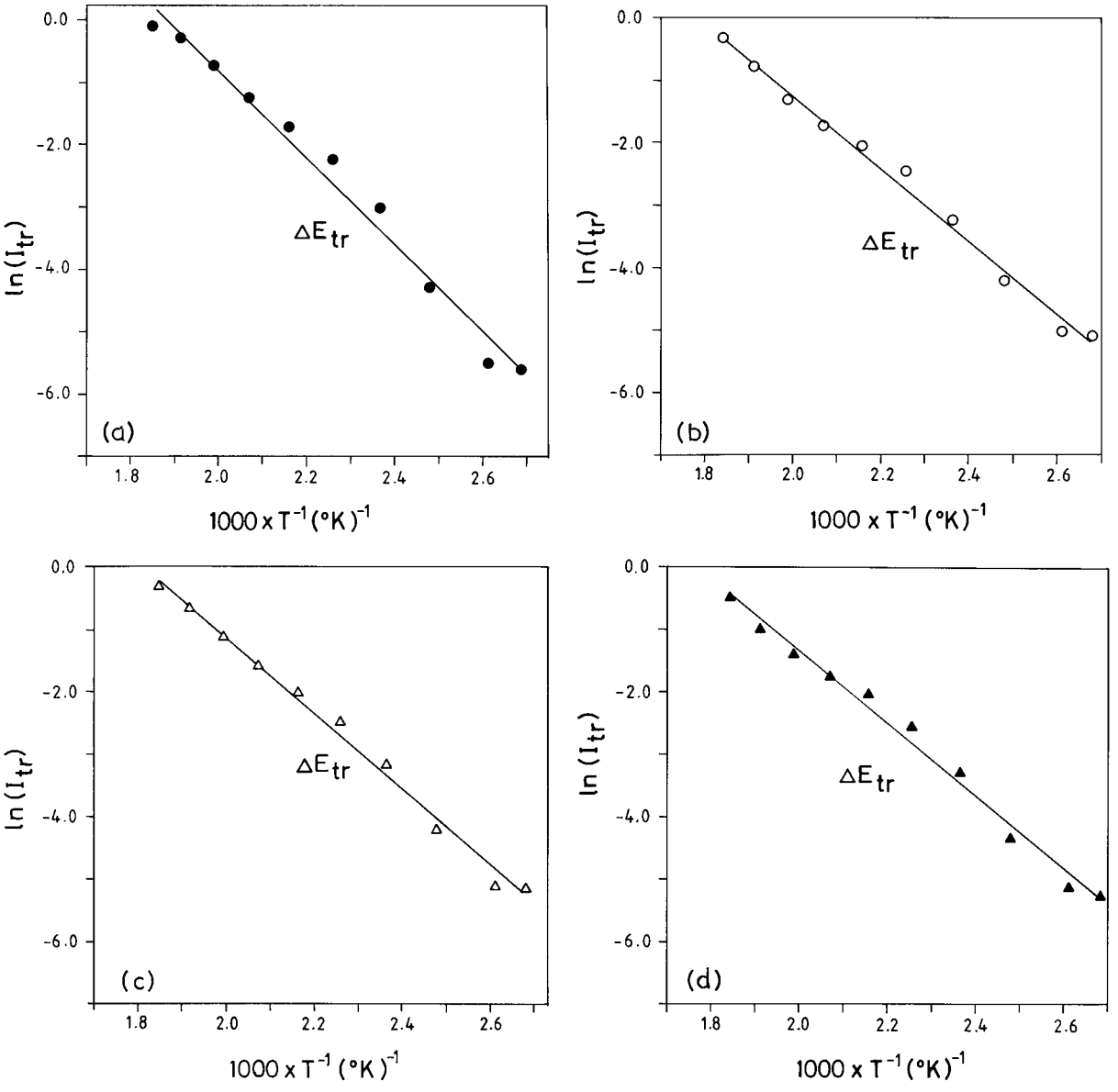

Figure 9 Logarithmic plots of the data in Figure 2(a) versus reverse of annealing temperature $(T)^{-1}$ for (a) 5-, (b) 10-, (c) 15-, and (d) 30-min time intervals.

K). The values of $B = 12.4 \times 10^3$ K and $B = 24.72 \times 10^3$ K for our system seems to be quite reasonable for our hard-latex particles and the measured values of B suggest that heptane has no plasticizing effect on the PMMA latex particles.

Crossing Density at Junction Surface

When the film samples were annealed at elevated temperatures in various time intervals, a continuous increase in the I_{tr} and I_{rf} intensities above 160°C were observed. The increase in I_{tr} and I_{rf} was already explained in the previous section, by the increase in the transparency of the latex film due to the disappearance of the particle–particle interfaces. As the annealing temperature is increased, some part of the polymer chains may cross the junction surface and particle boundaries start to disappear; as a result, the transmitted and reflected photon intensities increase due to the creation of high-quality, transparent mirror film.

To quantity these results, the Prager–Tirrell (PT) model[17] for the chain-crossing density was

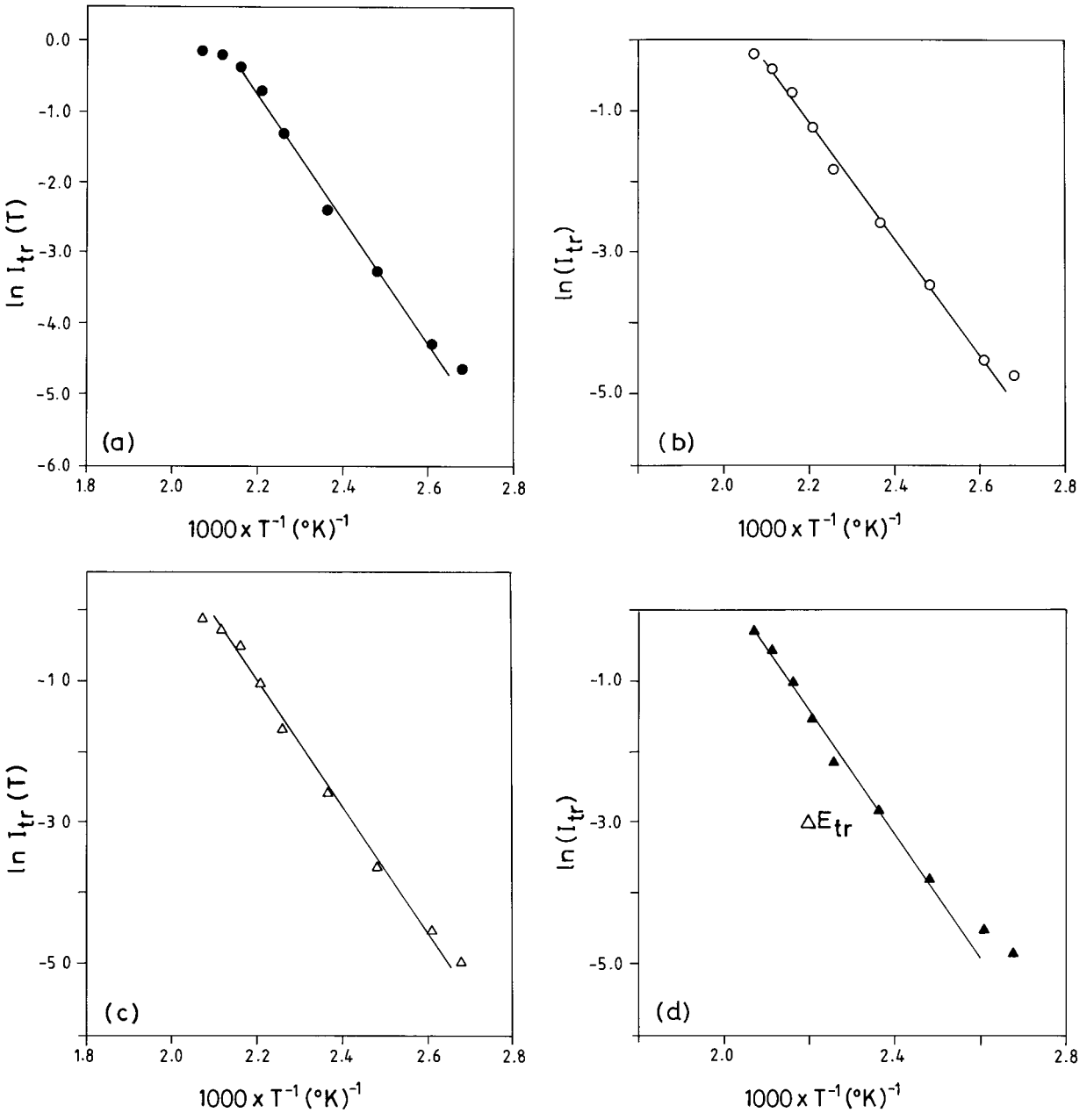

Figure 10 Logarithmic plots of the data in Figure 2(b) versus reverse of annealing temperature $(T)^{-1}$ for (a) 5-, (b) 10-, (c) 15-, and (d) 30-min time intervals.

employed. These authors used de Gennes's "reptation" model[29] to explain configurational relaxation at the polymer–polymer junction where each polymer chain is considered to be confined to a tube in which it executes a random back-and-forth motion. A homopolymer chain with N freely jointed segments of length L was considered by PT, which moves back and forth by one segment with a frequency ν. In time, the chain displaces down the tube by a number of segments, m. Here, $\nu/2$ is called the "diffusion coefficient" of m in a one-dimensional motion. PT calculated the probability of the net displacement with m during time t in the range of $n - \Delta$ to $n - (\Delta + d\Delta)$ segments. A Gaussian probability density was obtained for small times and large N. The total "crossing density" $\sigma(t)$ (chains per unit area) at the junction surface then was calculated from the contributions $\sigma_1(t)$ due to chains still retaining some portion of their initial tubes, plus a remain-

der, $\sigma_2(t)$. Here, the $\sigma_2(t)$ contribution comes from chains which have relaxed at least once. In terms of reduced time $\tau = 2\nu t/N^2$, the total crossing density can be written as

$$\sigma(\tau/\sigma(\infty) = 2\pi^{-1/2}\{\tau^{1/2} + 2\sum_{k=0}^{\infty}(-1)^n[\tau^{1/2} \times \exp(-k^2/\tau) - \pi^{-1/2}erfc(k/\tau^{1/2})] \quad (9)$$

For small τ values, the summation term of the above equation is very small and can be neglected, which then results in

$$\sigma(\tau)/\sigma(\infty) = 2\pi^{-1/2}\tau^{1/2} \quad (10)$$

This was predicted by de Gennes on the basis of scaling arguments.[29] To compare our results with the crossing density of the PT model, the temperature dependence of $\sigma(\tau)/\sigma(\infty)$ can be modeled by taking into account the following Arrhenius relation for the linear diffusion coefficient:

$$\nu = \nu_0 \exp(-\Delta E/kT) \quad (11)$$

Here, ΔE is defined as the activation energy for the back-and-forth motion. Combining eqs. (10) and (11), a useful relation is obtained as

$$\sigma(\tau)/\sigma)\infty = \text{Re } xp(-\Delta E/2kT) \quad (12)$$

where $R = (8\nu_0 t/\pi N^2)^{1/2}$ is a temperature-independent coefficient.

The increase in I_{tr} and I_{rf} is already related to the disappearance of particle–particle interfaces, that is, as annealing temperature is increased, more chains relaxed across the junction surface, and as a result, the crossing density increases. Now, it can be assumed that I_{tr} and I_{rf} is proportional to the crossing density $\sigma(T)$ and then phenomenological equations can be written as

$$I_{tr}(T)/\mathrm{I}_{tr}(\infty)=\mathrm{Rexp}(-\Delta\mathrm{E}_{tr}/2\mathrm{kT}) \quad (13a)$$

$$I\mathrm{rf}(T)/I\mathrm{rf}(\infty)=Rexp(-\Delta E\mathrm{rf}/2kT) \quad (13b)$$

Logarithmic plots of I_{tr} versus T^{-1} are presented in Figures 9 and 10 for HM and LM films for 5-, 10-, 15-, and 30-min annealing time intervals. The activation energies, ΔE_{tr} are produced by fitting the data to eq. (13(a) and the averaged values are 35.24 and 24.88 kcal/mol for LM and HM, respectively. Logarithmic plots of I_{rf} versus T^{-1} are presented on the left-hand side of Figures 7 and 8 for the LM and HM films for 30-, 15-, 10-, and 5-min annealing time intervals. The activation energies, ΔE_{rf}, are produced by fitting the data to eq. (13(b) and the averaged values are 47.13 and 18.17 kcal/mol for the LM and HM films, respectively. The measured ΔE_{tr} and ΔE_{rf} values are listed in Table I. Here, the smaller activation energies for the HM samples suggest that chain segments need less energy to execute a back-and-forth motion at the higher-temperature range than for LM samples. However, chain segments for the LM samples need greater energy to do the same motion at the lower-temperature region. The differences between the ΔE_{tr} and ΔE_{rf} values in the HM and LM samples most probably originate from the experimental positions in the unmodified and modified UVV techniques. This question will be answered in our future work. In conclusion, this work offers a simple technique (UVV) to study and measure the useful parameters during latex film formation by observing the surface and the bulk quality of films during the annealing processes.

REFERENCES

1. P. R. Sperry, B. S. Snyder, M. L. O'Dowd, and P. M. Lesko, *Langmuir,* **10,** 2619 (1994).
2. S. Mazur, in *Coalescence of Polymer Particles,* Polymer Powder Technology, M. Maukis and V. Rosenweig, Eds., Wiley, New York, 1996.
3. J. K. Mackenzie and R. Shuttleworth, *Proc. Phys. Soc.,* **62,** 838 (1946).
4. J. W. Vanderhoff, *Br. Polym. J.,* **2,** 161 (1970).
5. G. Kanig and H. Neff, *Colloid Polym. Sci.,* **256,** 1052 (1975).
6. Y. Wang, A. Kats, D. Juhue, M. A. Winnik, R. R. Shivers, and C. J. Dinsdale, *Langmuir,* **8,** 1435 (1992).
7. B. J. Roulstone, M. C. Wilkinson, J. Hearn, and A. J. Wilson, *Polym. Int.,* **24,** 87 (1991).
8. K. D. Kim, L. H. Sperling, and A. Klein, *Macromolecules,* **26,** 4624 (1993).
9. Ö. Pekcan, M. A. Winnik, and M. D. Croucher, *Macromolecules,* **23,** 2673 (1990).
10. Y. Wang, C. L. Zhao, and M. A. Winnik, *J. Chem. Phys.,* **95,** 2143 (1991).
11. Y. Wang and M. A. Winnik, *Macromolecules,* **26,** 3147 (1993).
12. Ö. Pekcan and M. Canpolat, *J. Appl. Polym. Sci.,* **59,** 277 (1996).

13. Ö. Pekcan, M. Canpolat, and A. Göçmen, *Polymer,* **34,** 3319 (1993).
14. M. Canpolat and O. Pekcan, *Polymer,* **36,** 4433 (1995).
15. Ö. Pekcan, *Trends Polym. Sci.,* **2,** 236 (1994).
16. M. Canpolat and Ö. Pekcan, *J. Polym. Sci. B Polym. Phys.,* **34,** 691 (1996).
17. S. Prager and M. Tirrell, *J. Chem. Phys.,* **75,** 5194 (1981).
18. M. A. Winnik, M. H. Hua, B. Hongham, B. Williamson, and M. D. Croucher, *Macromolecules,* **17,** 262 (1984).
19. Ö. Pekcan, M. A. Winnik, and M. D. Croucher, *Macromolecules,* **17,** 262 (1994).
20. Ö. Pekcan, M. A. Winnik, and M. D. Croucher, *Phys. Rev. Lett.,* **61,** 641 (1988).
21. Ö. Pekcan, *Chem. Phys. Lett.,* **20,** 198 (1992).
22. Ö. Pekcan and M. Canpolat, *J. Appl. Polym. Sci.,* **59,** 1699 (1996).
23. J. L. Keddie, P. Meredith, R. A. L. Jones, and A. M. Donald, in *Film Formation in Waterborne Coatings,* ACS Symposium Series 648, T. Provder, M. A. Winnik, and M. W. Urban, Eds., American Chemical Society, Washington, DC, 1996, pp. 332–348.
24. G. B. McKenna, in *Comprehensive Polymer Science,* Vol. 2, C. Booth and C. Price, Eds., Pergamon Press, Oxford, (1989).
25. H. Vogel, *Phys. Z.,* **22,** 645 (1925).
26. G. S. Fulcher, *J. Am. Ceram. Soc.,* **8,** 339 (1925).
27. D. W. Van Krevelen and P. J. Hoftyser, *Properties of Polymers: Their Estimation and Correlation with Chemical Structure,* Elsevier, Amsterdam, 1976, p. 343.
28. J. L. Keddie, P. Meredith, R. A. L. Jones, and A. M. Donald, *Macromolecules,* **28,** 2673 (1995).
29. P. G. de Gennes, *C.R. Acad. Sci. (Paris),* **291,** 219 (1980).